Research Square

Preprints are preliminary reports that have not undergone peer review.
They should not be considered conclusive, used to inform clinical practice,
or referenced by the media as validated information.

Increasing boreal fires reduce future global warming and sea ice loss

Edward Blanchard-Wrigglesworth

edwardbw@uw.edu

University of Washington https://orcid.org/0000-0002-2608-0868

Patricia DeRepentigny

Universite Catholique de Louvain https://orcid.org/0000-0002-0854-3793

Dargan Frierson

University of Washington

Physical Sciences - Article

Keywords:

Posted Date: December 4th, 2024

DOI: https://doi.org/10.21203/rs.3.rs-5486231/v2

License: This work is licensed under a Creative Commons Attribution 4.0 International License.
Read Full License

Additional Declarations: The authors declare no competing interests.

Increasing boreal fires reduce future global warming and sea ice loss

Edward Blanchard-Wrigglesworth[1*], Patricia DeRepentigny[2], Dargan Frierson[1]

[1]Department of Atmospheric and Climate Science, University of Washington, Seattle, WA, USA

[2]Earth and Climate Research Center (ELIC), Earth and Life Institute (ELI), Université catholique de Louvain (UCLouvain), Louvain-la-Neuve, Belgium

*Corresponding author: Edward Blanchard-Wrigglesworth, edwardbw@uw.edu, Department of Atmospheric and Climate Science, University of Washington, Seattle, WA, USA

Keywords Global warming | Boreal fires | CMIP7

Classification Physical Sciences | Earth, Atmospheric, and Planetary Sciences

Pre-print server Deposited to Research Square. The preprint is licensed under a CC BY 4.0 License.

Abstract

Biomass burning can affect climate via the emission of aerosols and their subsequent impact on radiation, cloud microphysics, and surface and atmospheric albedo[1,2]. Boreal biomass burning emissions have strongly increased during the last decade and are expected to continue increasing as the climate warms[3–6]. Climate models simulate aerosol processes, yet historical and future Coupled Model Intercomparison Project (CMIP) simulations have no active fire component, and biomass burning emissions are prescribed as external forcings. Here we show that CMIP6 used future boreal emission scenarios with unrealistic near-zero trends that have a large impact on climate trends. By running sensitivity experiments with ramped up boreal emissions based on observed trends, we find that increasing boreal emissions reduce global warming by 12% and Arctic warming by 38%, reducing the loss of sea ice. Tropical precipitation shifts southward as a result of the hemispheric difference in boreal aerosol forcing and subsequent temperature response[7]. These changes stem from the impact of aerosols on clouds, increasing cloud droplet number concentration, cloud optical depth, and low cloud cover, reducing surface shortwave flux over northern latitudes. Our results highlight the importance of realistic boreal emissions in climate model simulations and the need for improved understanding of boreal emission trends and aerosol-climate interactions.

Significance statement

Over the past two decades, boreal biomass burning emissions (BBEs) have increased dramatically, and are expected to continue increasing. In contrast, CMIP6 models prescribe a future (2015-2100) boreal BBE scenario with low values and near-zero trends. To assess if the difference between observed and prescribed boreal BBE forcing has a climate impact, we produced new simulations using CESM2 with standard CMIP6 forcings, but increasing boreal BBEs based on observations. The increase in boreal BBEs slows down global warming by 12%, Arctic warming by 38%, reducing sea ice loss, and shifts tropical precipitation southward. These impacts highlight the importance that future boreal fires may have for climate projections, and motivate revising the design of boreal

BBEs for the upcoming CMIP7.

Main

Aerosols (in particular their sulfate component) generally have a negative radiative forcing (cooling) effect due to aerosol scattering of solar radiation[2] and via aerosol-cloud interactions that increase cloud condensation nuclei and cloud optical depth[8,9]. In contrast, black carbon (BC), mineral dust and other absorbing aerosol components can lead to a positive (warming) forcing in the Arctic due to absorption of solar radiation and the reduction of surface albedo when deposited on the snow/ice surface[10–12]. In addition, the radiative impact of airborne BC in the Arctic may be elevation-dependent, with BC at the surface or the lower (upper) atmospheric layers leading to warming (cooling)[13], and location-dependent, with some results showing that Arctic BC leads to Arctic cooling while northern mid-latitude BC leads to Arctic warming[14].

While current climate models participating in the Coupled Model Intercomparison Project (CMIP) simulate these aerosol processes, these models do not have active fire components, meaning that fires do not occur as a result of the interaction between different components of the climate system, and biomass burning emissions are instead prescribed as an external forcing. In the most recent CMIP generation (CMIP6), monthly and spatially varying satellite-based estimates of biomass burning emissions (BBEs) are based on the Global Fire Emission Database (GFED) over 1997–2014 and proxy-reconstructed BBEs prior to 1997[15], which have smaller interannual variability in BBEs than the satellite-based estimates (Figure 1A). For future scenarios, prescribed BBEs originate from integrated assessment models to produce a dataset of harmonized emissions trajectories over 2015–2100[16,17], which amounts to a near-constant 0.12 Tg C/yr of black carbon (BC) over the boreal region (56°N–70°N; Figure 1A). The enhanced interannual variability in prescribed BBEs over the GFED period has been shown to have a significant climate impact on historical CMIP6 simulations, with an acceleration of global warming and sea ice loss simulated over 1997–2014 as well as the amplification of the hydrological cycle poleward of 40°N[9,18,19]. This is due to the non-linear relationship between BBEs and their radiative impacts through aerosol-cloud interactions, as

years with anomalously low BBEs have more of a positive radiative forcing impact compared to the negative radiative forcing during years with anomalously high BBEs.

Earlier research postulated that the Arctic atmosphere may become cleaner in the future, especially during the cold season as the climate warms and precipitation increases[20–22], leading to enhanced wet deposition and aerosol scavenging. Past literature on changes in BC transport to the Arctic has generally not considered the potential impact of an increase in boreal BBEs[1], yet recent years have been marked by record-breaking boreal fires, particularly over Siberia[3–6] and Canada[23]. The increase in BBEs has been attributed to earlier spring snowmelt, summer sea ice loss, warmer summers, increases in vapor pressure deficit, drier soils, and increased occurrence of atmospheric blocking patterns that lead both to warm and dry weather as well as convection which can cause lightning and fire ignitions[5,24–26]. As all these factors are expected to amplify with global warming, boreal fires are also expected to keep increasing in frequency and intensity[23,25].

In this paper, we compare observed BBEs over 1997–2023 to the prescribed BBEs used in CMIP6 and find that boreal BBEs have drastically increased over the last ten years compared to the early 21st century CMIP6 BBEs. To assess the impact of this divergence in boreal BBEs between observations and those prescribed in CMIP6, we run new simulations with the CESM2 forced with an increase in boreal BBEs over 2015–2060 that reflects recent observed trends and the predicted increase in future boreal fires. We find that enhanced boreal BBEs produce a negative radiative forcing that slows down future warming especially in the Arctic and boreal region, while also affecting tropical precipitation patterns.

Results

Increase in observed boreal biomass burning emissions

Boreal BBEs have sharply increased over the last decade, from an average BC emission of 0.10 Tg C/yr over 1997–2014 to 0.26 Tg C/yr over 2015–2023 (Figure 1A, we use BC as a proxy for total BBEs, see methods). Recent years have recorded increasingly extreme

values, with 0.28 Tg C/yr of BC in 2019, 0.45 Tg C/yr in 2021, and 0.68 Tg C/yr in 2023. Zonally-averaged, the boreal region is the only region that has seen a significant increase in BBEs over 1997–2023 (Figure 1D). In contrast, BBEs globally and south of 56°N have trended negative since the late 1990s (Figure 1B–C)[27,28], mainly driven by declining BBEs over the tropics associated to a decrease in grassland and savanna area related to agricultural expansion[27]. As a result, the contribution of boreal BBEs to global BBEs has starkly increased over 1997–2023, from contributing ∼4% of global emissions over 1997–2010 to over 10% almost every year since 2010 and peaking at almost 30% in 2023 (Figure S1).

Differentiating observed boreal BC BBEs between North America and Eurasia shows that the remarkable increase is both due to an increase in boreal emissions from Eurasia and North America, with fires in eastern Siberia driving the record emissions in 2019 and 2021 and the 2023 wildfire season in Canada driving the record value that year (Figure 1E). Over the long term, the increasing trend is statistically more robust over Eurasia, as the 1997–2023 trend calculated over North America is strongly influenced by the highly anomalous value in 2023. Boreal BBE trends of BC over Eurasia are ∼0.05 Tg C/yr/decade over both 1997–2022 and 1997–2023, while trends over North America are 0.02 Tg C/yr/decade over 1997–2022 and 0.06 Tg C/yr/decade over 1997–2023 (Figure 1E).

In contrast to recent observed boreal BBEs, the CMIP6 forcing uses a near-constant scenario, with 0.12 Tg C/yr of BC from boreal BBEs from 2015 onwards (as was the case in CMIP5[18]) such that, in every year since 2015, observed boreal BBEs are greater than those used in CMIP6 (Figure 1A). Outside the boreal region, prescribed CMIP6 BBEs are within the observed range since 2015 (Figure 1B,C), highlighting the boreal region as the main source of diverging pathways in BBEs between observations and CMIP6 future simulations. The increase in boreal fires has led to an increase in aerosol optical depth during the summer over the boreal region and the Arctic over the past two decades (Figure 1G-I). Averaged over 56°N-70°N, mean JJA AOD has doubled from an average 0.039 in 2003–2014 to 0.078 in 2019–2023. In the Arctic (70°N-86°N), AOD has more than tripled, from 0.015 in 2003–2014 to 0.056 in 2019–2023. Given the importance of

aerosols for climate, this discrepancy in boreal BBEs between observations and CMIP6 in the future could lead to important climate impacts that are currently not captured in the most recent modeling assessments.

Model simulations forced with increase in boreal BBEs

Given that the causes of the recent increase in boreal BBEs (summer warming, loss of spring snow cover, loss of Arctic sea ice)[23,25,26] are expected to amplify under future warming, it is also expected that boreal fires will continue to increase both in frequency and intensity[25,29,30]. To test the impact of an increase in boreal BBEs on future climate, we run new model simulations (hereafter named BorealFire) using the fully-coupled CESM2 climate model over 2015–2060 with standard CMIP6 SSP3-7.0 forcing except for boreal BBEs, which are updated over 2015–2023 based on observations and extended to 2060 based on recent observed trends (see Methods for more details). Total boreal and global BC BBEs in BorealFire are shown in Figure 1A,B and regional boreal BBEs in Figure S2. Outside the boreal region (56°N–70°N), BBEs in BorealFire are kept unchanged relative to CMIP6. While there is an exponential relationship between summer temperature and boreal fires[25], future boreal fire projections based solely on future temperature increase do not take into consideration the negative fuel-availability feedback. Thus a linear increase in boreal BBEs, while more conservative than an exponential increase, may be a more realistic approach. In addition, applying a linear projection results in values over 2020–2060 that, until the late 2050s, are below the observed 2023 value, meaning the prescribed BBEs in BorealFire are within the realm of past boreal BBEs.

The increase in BBEs in BorealFire occurs during the boreal fire season (May through September), and represents a 4-fold increase averaged over 2020–2060 relative to the CMIP6 forcing used for the same period (0.49 Tg C compared to 0.12 Tg C of BC; Figure 1F). The resulting aerosol burdens are strongly amplified over the boreal region in summer in BorealFire (see Figure 2A-C for particular organic matter [POM], sulfate [SO_4], and BC), while changes in other seasons are much smaller or insignificant (Figures S3–S5). The difference between BorealFire and CESM2-LE not only highlights the

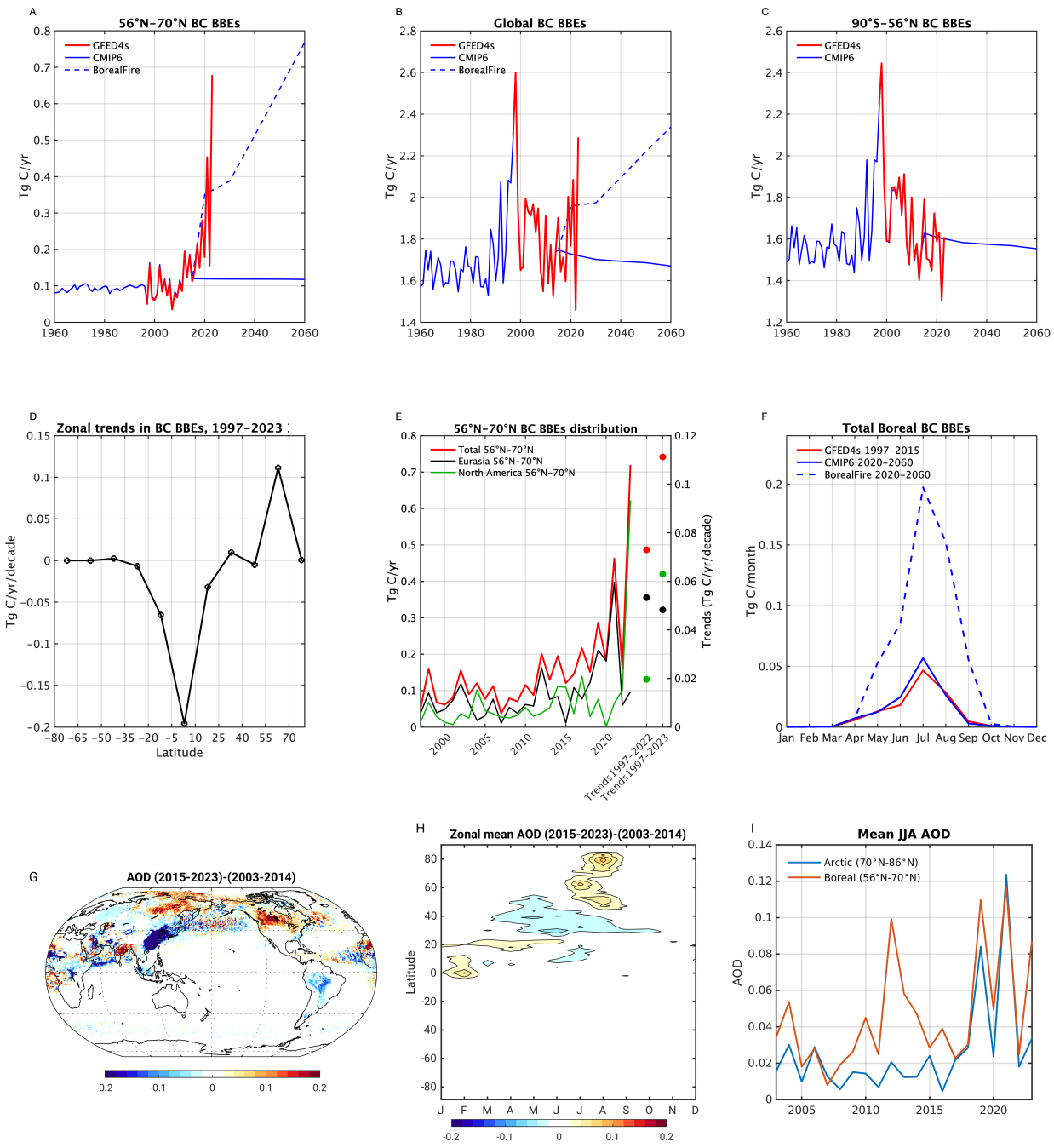


Fig. 1 | **Evolution of observed, CMIP6, and BorealFire BBEs.** (A) BC from BBEs over 56°N–70°N in GFED (red), prescribed in CMIP6 experiments (blue), and prescribed in our sensitivity experiment BorealFire (dashed blue). (B–C) As in (A), but for BBEs globally and south of 56°N, respectively. (D) Observed zonal trends in BC BBEs over 1997–2023, calculated in 15°latitudinal bands. (E) Total BC from BBEs over 56°N–70°N (red) differentiated between Eurasian (black) and North American BBEs (purple), with 1997–2022 and 1997–2023 trends shown by dots and associated values on the right y-axis. (F) Monthly-mean BC from boreal BBEs over 1997–2015 (red), CMIP6 over 2020–2060 (blue), and BorealFire over 2020–2060 (dashed blue). Observed (H) summer and (G) year-round zonal-mean AOD difference between 2015–2023 and 2003–2014, and (I) mean Arctic and boreal summer (JJA) AOD, 2003–2023.

large increase in burdens where fires occur but also that those aerosols are advected downstream beyond the boreal BBE source regions (East Siberia and Canada), resulting in enhanced aerosol optical depth during the summer north of 40 °N (Figure 2D-F). The simulated changes in summer AOD over the northern high latitudes are comparable to the observed recent increase in AOD associated with increasing boreal fires (cf Figure 1G-I).

The increase in aerosol burdens in BorealFire results in slower warming rates over the high northern and mid latitudes and North Pacific and North Atlantic, which leads to a significant weakening of the global warming trend (Figure 3). The ensemble-mean global warming trend over 2015–2060 in BorealFire (0.32°C/decade) is weaker relative to CESM2-LE (0.37°C/decade), a reduction of 12%, and a statistically robust ensemble-mean cooling signal emerges by 2030. Over the Arctic (70°N–90°N), warming rates in BorealFire are 38 % weaker (0.49°C/decade) those in CESM2-LE (0.78°C/decade, Figure 3B), and a statistically robust ensemble-mean cooling signal emerges by the early 2020s. Arctic Amplification (defined as the ratio of Arctic to global warming trends) is reduced from 2.1 in CESM2-LE to 1.5 in BorealFire. Damped warming in BorealFire extends southward to about 40°N over Asia and North America, and further south over the north Pacific and North Atlantic. The temperature response over the North Pacific tends to be stronger than that over the North Atlantic. Over much of the Southern Hemisphere, where aerosol burdens are not affected by boreal BBEs, temperature trends in BorealFire are comparable to CESM2-LE trends (Figure 3C-E).

Seasonally-distinct temperature trends emerge in BorealFire relative to the CESM2-LE (Figure 4A-D). During summer, the largest surface temperature trend differences are about 0.2–0.4°C/decade cooler in BorealFire relative to the CESM2-LE, located over the regions of the largest increase in prescribed BBEs and summer aerosol burden increase (i.e., Siberia and northern Canada) and in their vicinity over land (Figure 4C). During fall and winter, temperature trend differences are greatest over the Arctic Ocean (-0.5°C/decade in BorealFire relative to the CESM2-LE), while spring trend differences are similar in spatial pattern but weaker in amplitude than in other seasons. In the North Pacific, temperature trends are significantly more negative throughout the year.

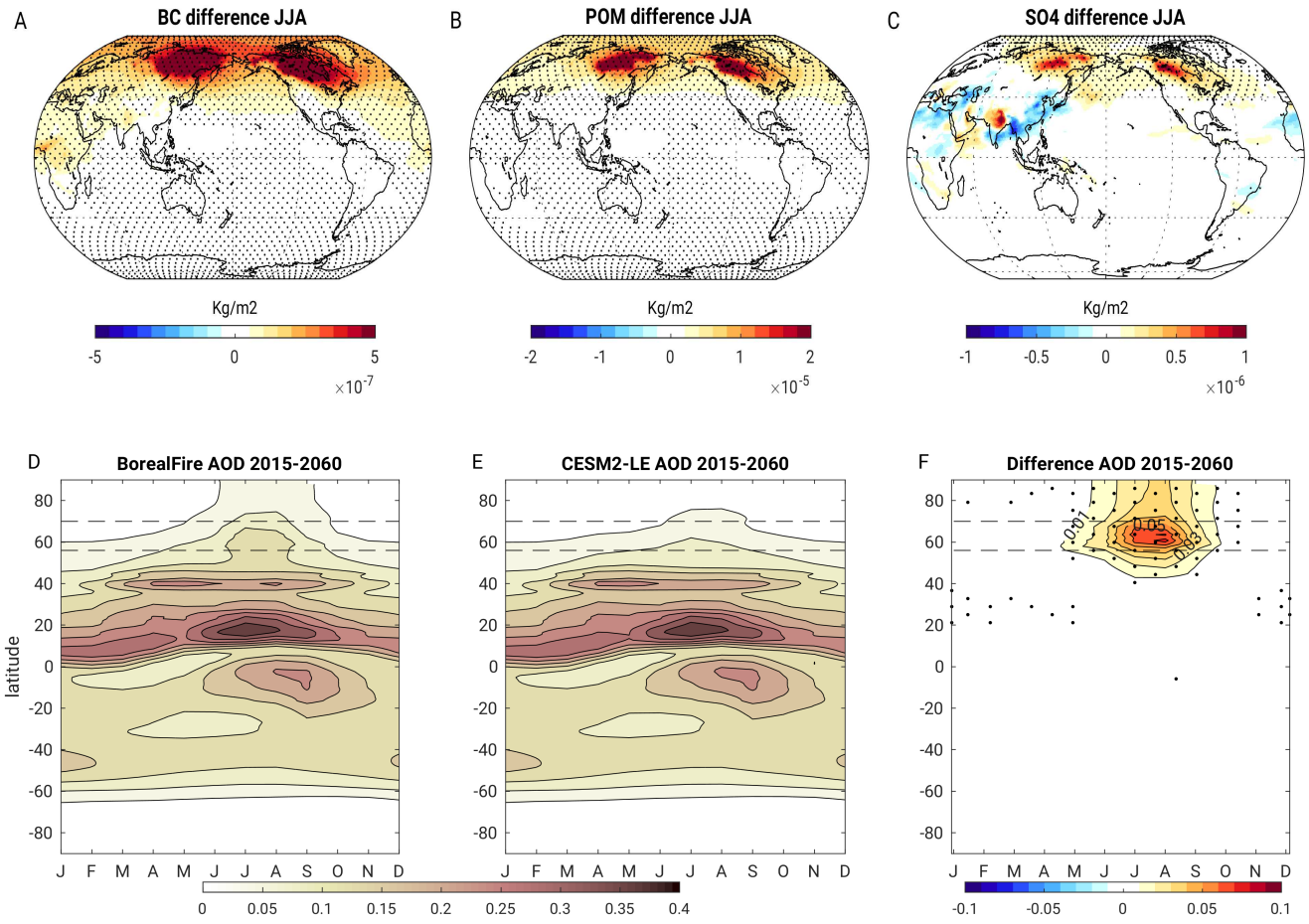


Fig. 2 | **Changes in aerosol distribution with increased future boreal fires.** Difference (BorealFire – CESM2-LE) in summer (JJA) column-integrated burden averaged over 2015–2060 for (A–C) BC, POM, and SO_4. Zonally-averaged aerosol optical depth (AOD) in (D) BorealFire, (E) CESM2-LE, and (F) the difference between the two. The dashed lines indicate the boreal region (56°N–70°N). Regions where the difference is greater than the CESM2-LE ensemble standard error are stippled.

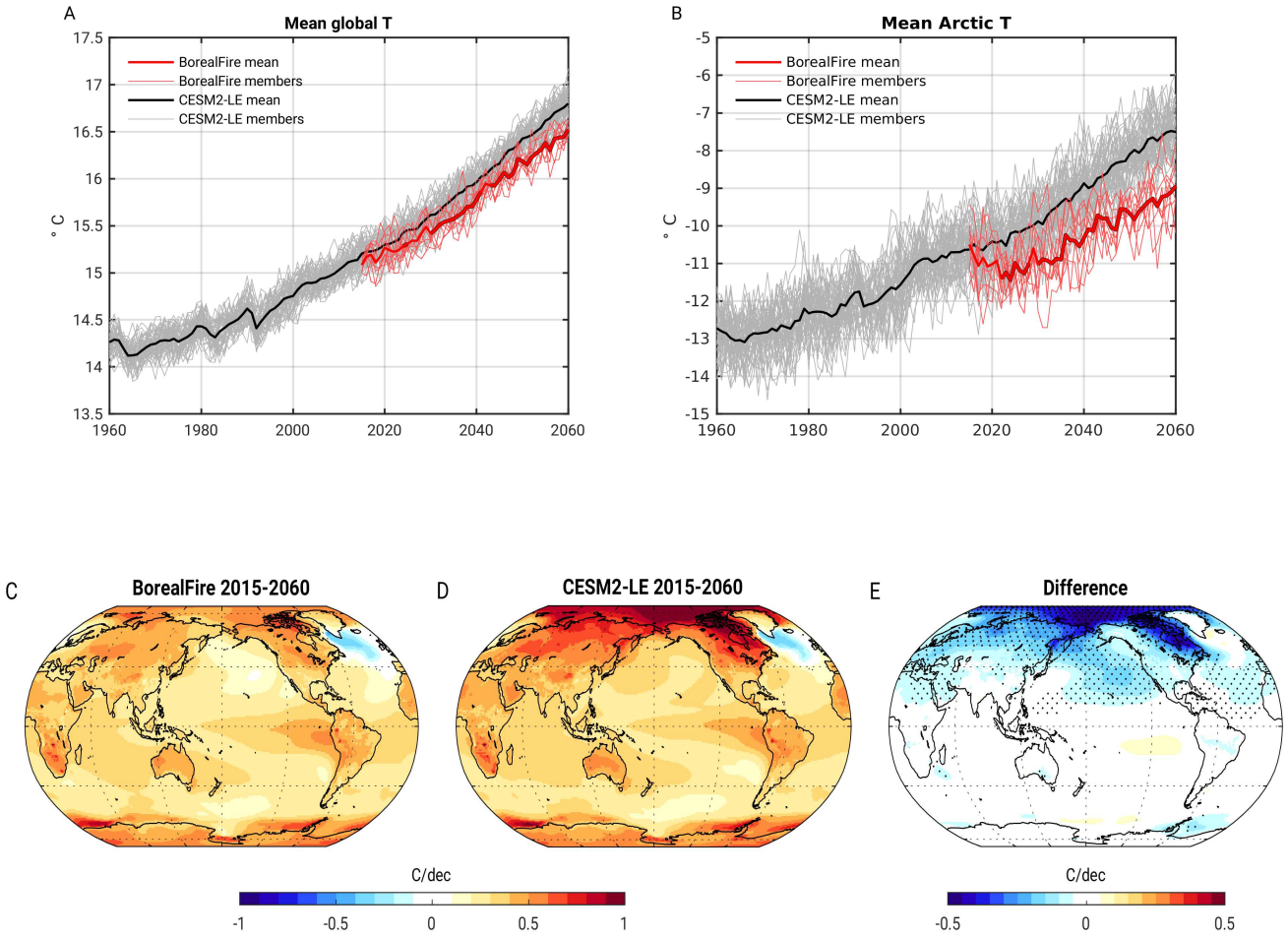


Fig. 3 | **Future warming rates under increased future boreal fires.** (A) Evolution of global mean surface temperature in BorealFire (red) and CESM2-LE (black), with individual members shown as thin lines and the ensemble mean indicated by the thick line. The BorealFire ensemble mean line is highlighted with a black border during years when its difference with the CESM2-LE ensemble mean is greater than the CESM2-LE ensemble standard error. (B) As in (A), but for Arctic temperature (70°N–90°N). Linear temperature trend over 2015–2060 in °C per decade in (C) BorealFire, (D) CESM2-LE, and (E) the difference between the two. Regions where the difference in trends is greater than the CESM2-LE ensemble standard error are stippled.

While temperature trends over most of the Southern Hemisphere are unaffected by the increase in boreal BBEs, there is a modest relative cooling signal in austral winter and spring (JJA and SON) in the Pacific sector of the Southern Ocean (Figure 4C,D). Averaged zonally, temperature differences are greatest near the surface over the Arctic in fall and winter whereas during summer the cooling is focused over 55°N–70°N and extends upward into the troposphere more clearly than in other seasons (Figure 4E–H). In summer, the cooling in the high Arctic peaks around the top of the boundary layer (800–900 mb), and is more muted at the surface. The upper troposphere in the tropics and northern sub-tropics tends to cool especially in summer and fall (Figure 4G,H). These vertical temperature change patterns are likely a direct response to the aerosol forcing during summer and to the sea ice/sea-surface temperature change forcings[31], which themselves are driven by the summer aerosol forcing. We discuss the processes behind these aerosol-climate interactions in more detail below.

In addition to changes in global and regional warming patterns, we also find impacts on other key aspects of the climate system as a result of increased boreal fires. Precipitation decreases in the northern high latitudes, while tropical precipitation shifts southward (Figure 5A, B). The tropical changes are consistent with the hemispheric temperature differences in Figure 3 and a migration of the ITCZ away from the anomalously cooler hemisphere (i.e., southward)[7]. However, the changes in tropical precipitation, relative to its mean state, are basin-dependent. In the Indian Ocean, there is a southward shift of the ITCZ, whereas in the Pacfic, the ITCZ narrows, while the South West Pacific ITCZ strengthens and expands eastward. In the Atlantic, the ITCZ weakens, but shows no increase to the south. In the northern high latitudes, precipitation decreases, which is consistent with the relatively cooler Arctic temperatures in BorealFire (a warmer Arctic is a wetter Arctic[32,33]). In addition, summer precipitation decreases in the regions of enhanced boreal BBEs over Siberia and Canada (Figure S6). In the Arctic, sea ice loss is strongly impacted by the increase in prescribed future BBEs. In BorealFire, the mean Arctic sea ice extent recovers between 2015 and 2025 and declines over 2025–2060 at a slower pace relative to the CESM2-LE (Figure 5C). The September sea ice cover (the month of the annual minimum), which is mostly lost in CESM2-LE by 2050,

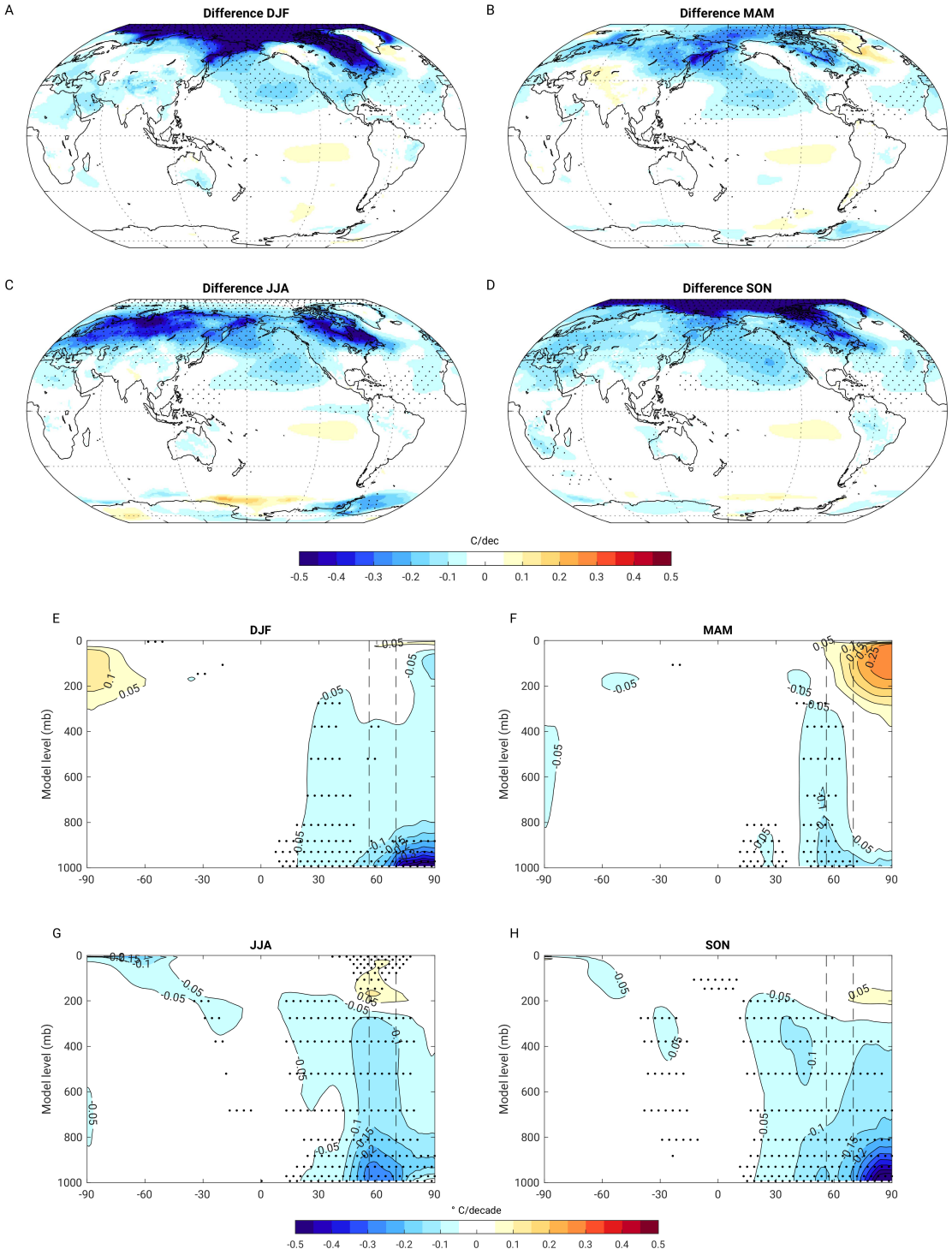


Fig. 4 | **Seasonal and vertical distribution of temperature changes.** Differences in (A–D) seasonal surface temperature trends and (E–H) seasonal zonal-mean temperature trends between Boreal Fire and the CESM2-LE over 2015–2060 in °C per decade.

is more resilient in BorealFire, with a sea ice extent of 2 million km^2 remaining by 2060 (Figure 5D). Changes in atmospheric circulation in the middle and high latitudes, as reflected by changes in mean sea level pressure (SLP), are mostly insignificant (Figure S7), with the exception of slightly higher SLP over the Arctic Ocean in BorealFire during the cold season, reflecting a known circulation response in CESM2 to colder Arctic surface temperatures and greater sea ice coverage in BorealFire[34].

Why do enhanced boreal BB emissions lead to weaker Northern Hemisphere warming? In Figure 6, we show the summer zonal mean differences in aerosol concentration number and cloud optical depth between BorealFire and CESM2-LE, and the annual-mean differences in cloud droplet number, low cloud cover, and surface net shortwave flux (seasonal differences for these variables are shown in Figures S8–S10). During summer (JJA), aerosol concentration number in BorealFire is significantly larger over the boreal region, with the maximum difference found near the surface between 60°N–70°N, while over the Arctic the difference between both ensembles peaks at around 850 hPa (Figure 6A). The changes in cloud optical depth (Figure 6B) and cloud droplet number (Figure S8) mirror those in aerosol concentration number, with more optically thick clouds and higher cloud droplet numbers in BorealFire in summer over the boreal region, the Arctic, and the northeast Pacific and Atlantic. In addition, low cloud fraction increases, especially over the northeast Pacific and Atlantic (Figure S7). During the other seasons, differences are much smaller, with the increase more limited to the boreal region. As a result of these aerosol-cloud interactions, annual-mean net shortwave fluxes at the surface are reduced over the high northern latitudes and over the North Pacific and North Atlantic. The annual-mean shortwave flux differences result mainly from summer differences (Figure S8) that are driven by increased cloud optical depth and in some regions by increased low cloud cover (especially over the Pacific and Atlantic). In contrast, the annual-mean low cloud cover over the Arctic Ocean decreases, but this change is driven by the cold season changes (Figure S7). During summer, Arctic low cloud cover is unchanged in BorealFire relative to CESM2-LE, which has a summer low cloud climatology close to full coverage. The summer increase in cloud optical depth at around 850 mb over the Arctic Ocean (Figure 6B) and corresponding cooling at this

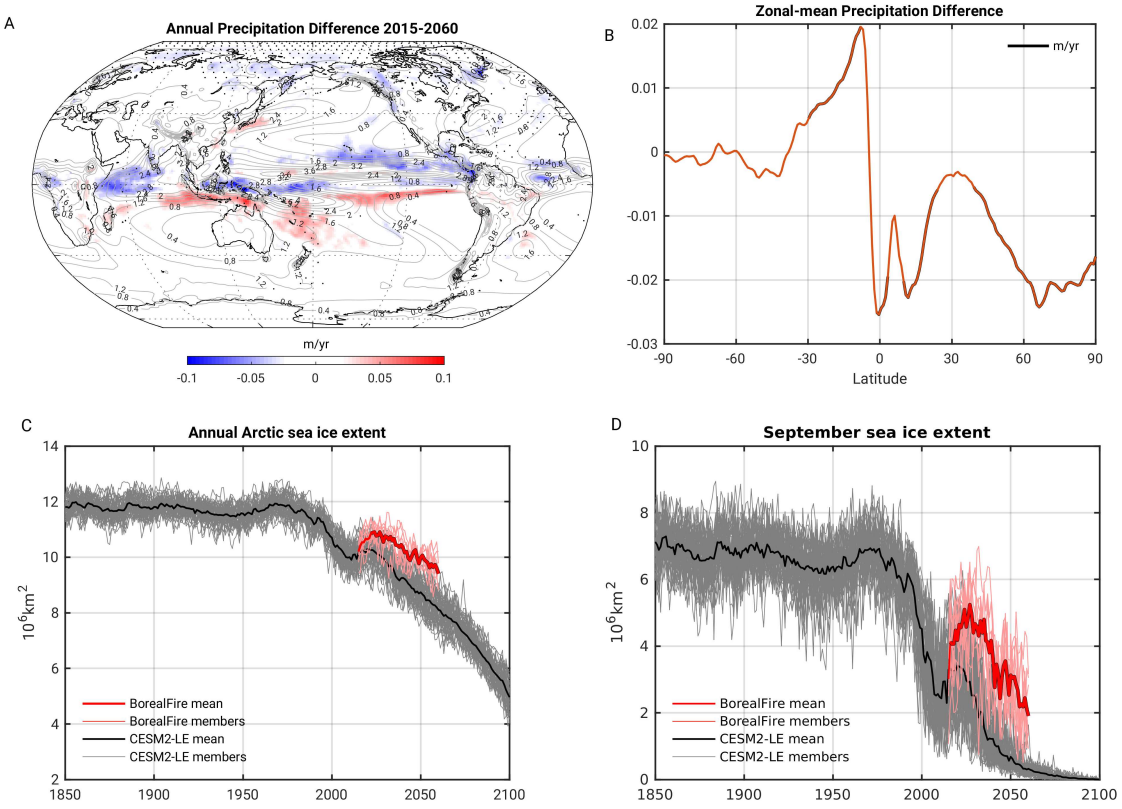


Fig. 5 | **Impact on precipitation and Arctic sea ice.** (A) Mean annual precipitation difference over 2015–2060 in m/yr between BorealFire and CESM2-LE, with gray contours showing the 2015–2060 climatology in CESM2-LE, and (B) zonal-mean difference. (C) Annual mean and (D) September sea ice extent in BorealFire (red) and CESM2-LE (black), with individual members shown as thin lines and the ensemble mean indicated by the bold line. The BorealFire ensemble mean line is highlighted with a black border during years when its difference with the CESM2-LE ensemble mean is greater than the CESM2-LE ensemble standard error.

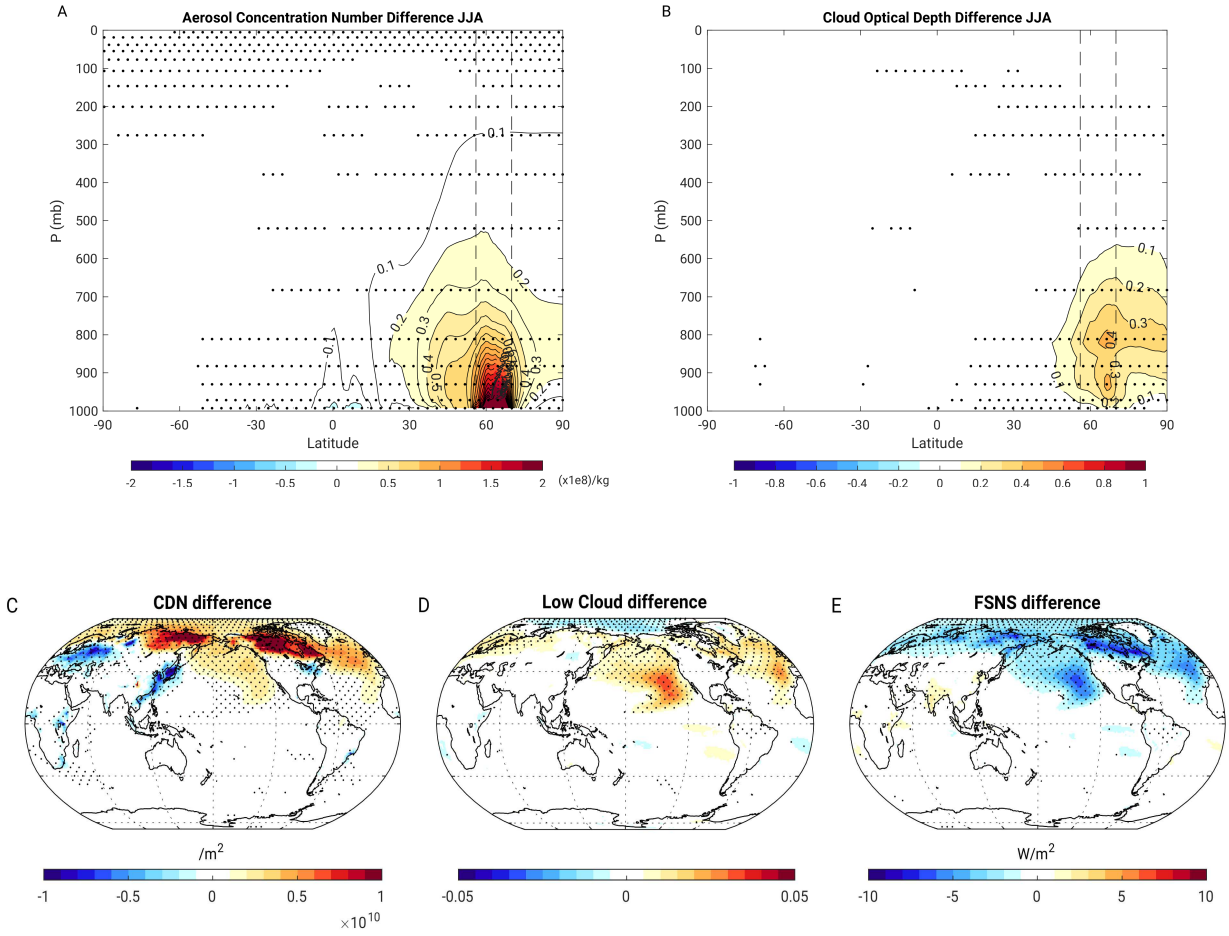


Fig. 6 | **Impact on aerosols, clouds and radiation.** Summer (JJA) zonal-mean differences in (A) aerosol concentration number and (B) cloud optical depth, and annual-mean differences in (C) cloud droplet number, (D) low cloud fraction and (E) net shortwave flux at the surface (FSNS), between BorealFire and CESM2-LE over 2015–2060.

elevation during summer (Figure 4B) lead to an increase in summer snowfall relative to CESM2-LE (not shown) which, together with the greater sea ice extent discussed above (Figure 5B), increases the surface albedo over sea ice (Figure S9), thereby reducing net surface shortwave fluxes.

Discussion

Boreal biomass burning emissions have shown a significant increase over the last decade, from an average of 0.10 Tg C/yr of BC over 1997–2014 to 0.26 Tg C/yr of BC over 2015–

2023. Recent years have recorded increasingly extreme values, with 0.28 Tg C/yr in 2019, 0.45 Tg C/yr in 2021, and 0.68 Tg C/yr in 2023. The increase in observed boreal BBEs result from an increase in emissions from Siberia and Canada, which have been attributed to significant summer warming, spring snow loss, summer sea ice loss, increases in vapor pressure deficit, and convective atmospheric patterns that enhance ignition[5,23,25,26]. This observed increase in boreal BBEs is not replicated by the forcing emissions scenario used in CMIP6, which use a near-zero trend over 2015–2100 based on a pre-2015 observed climatology.

Projected summer warming, declining spring snow cover, and permafrost thaw in coming decades will likely lead to a continued increase of boreal BBEs[25,26,35], and thus the divergence between observed boreal BBEs and those prescribed in 21st century CMIP6 runs is likely to remain in the near future. Given the importance of BBEs to global and Arctic climate[8,9,18,19], we assessed the impact of increased BBEs over 2015–2060 in CESM2 by forcing the model with new boreal emissions based on observations and their linear extrapolation. We found a significant impact on global climate, with increased boreal BBEs leading to damped global warming (0.32°C/decade versus 0.37°C/decade in CESM2-LE) and Arctic warming (0.49 °C/decade versus 0.78 °C/decade in CESM2-LE), a decline in the rate of Arctic sea ice loss, and a southward shift in tropical precipitation. These climate impacts result from the increase in aerosol concentration number, which results in larger cloud droplet number, cloud optical depth, and reduced shortwave flux at the surface over the mid and high northern latitudes over land and over the North Pacific and North Atlantic. These spatial patterns are similar to those found in response to historical BBE variability over 1997–2014 in CESM2[9].

While the aerosol burden differences and their cloud and radiation impacts are greatest in the summer (because of the increase in boreal BBEs during the summer fire season), the temperature response is greatest over the Arctic in fall and winter. This asynchronous timing in the response relative to the radiative forcing anomaly associated with BBEs is consistent with the seasonal modulation of Arctic Amplification[36]; Arctic summer surface temperatures are constrained to the freezing point over the melting sea ice surface, attenuating summer surface temperature change, yet sea ice melt is re-

duced due to the smaller shortwave flux. The larger and thicker sea ice cover persists into fall and winter[37], leading to cooler surface temperature as the thicker sea ice cover insulates the atmosphere from ocean heat. While surface temperature impacts over the tropics and Southern Hemisphere are not significant, tropical precipitation is impacted, shifting slightly south in BorealFire relative to the CESM2-LE. This shift illustrates a southward shift of the ITCZ, a known response to hemispheric differences in temperature gradients related to high latitude ice cover changes[7], and similar to the response in precipitation to historical BBEs variability in CESM2[19].

The results shown here highlight the importance in assessing the impact of realistic boreal BBEs on current state-of-the-art GCMs, as well as the need to improve our understanding of trends in boreal forest fires and the physical processes that determine the impact of boreal BBE aerosols on climate[18,38]. Further work should also explore feedbacks between change in land type after fires (which are kept constant in our experiments) and the overall climate response to fire aerosol emissions, as fires affect surface albedo, energy and water fluxes and local surface temperature responses[39,40]. Our results showing the impact of increasing boreal fires on Arctic climate may be a contributing factor to the recent slowdown in Arctic amplification[41], and imply that if global and Arctic warming trends are weakened by increasing boreal BBEs, any posterior reduction in future boreal BBEs, as a consequence of forest management or the negative fuel-availabilty feedback, may in turn contribute to a posterior acceleration of global and Arctic warming. Given the divergence in observed and prescribed boreal BBEs, and their simulated impact on climate, we strongly argue that CMIP7 model simulations should consider projections of increased boreal BBEs in future 21st century simulations.

Methods

For the timeseries analysis in Figures 1 and S1, we show BC from BBE emissions as a proxy for total BBEs, which over boreal and temperate forest are estimated as a fixed factor of total dry matter burned[15], and note that all other prescribed BB emissions (dimethyl sulfide, primary organic matter, sulfur dioxide, sulfate aerosols, and secondary organic aerosols), when normalized, follow the same time evolution as BC (Figure S1).

To inspect trends in observed boreal BBEs, we use the Global Fire Emission Database version 4 (GFED4s)[42,43] over 1997–2023. To inspect trends in observed aerosol optical depth, we use the AOD 550 Dark Target Deep Blue Combined Mean, available from NASA MODIS/Aqua Aerosol Cloud Water Vapor Ozone Monthly level 3 Global product over 2003–2023. We assess the climate impact of increasing boreal BBEs with the CESM2 model[44]. We run a new set of simulations (hereafter named BorealFire) over 2015–2060, branched off from existing CESM2 CMIP6 and CESM2-Large Ensemble (CESM2-LE)[45] members in 2015. These sensitivity experiments are forced with the CMIP6 Shared Socioeconomic Pathway 370 (SSP3-7.0, representing the medium to high end of the range of plausible future forcing pathways) scenario emissions except for boreal BBEs which are taken from GFED4s values over 2016–2023 and follow an extrapolation of the observed 1997–2023 linear trend for the period 2023–2060 for each grid cell and each month. For the 21st century simulations, the standard CESM2 model prescribes BBEs at decadal timesteps (2020, 2030, 2040, etc.) and linearly interpolates between them. To capture the large observed values over 2019–2023, we use the GFED4s BBEs averaged over 2019–2023 for the first prescribed timestep (2020) in our sensitivity experiments BorealFire. For the 2030–2060 timesteps, we prescribe new boreal BBEs by calculating the linear trend of observed boreal BBEs over 1997–2023 at each grid cell and month and extrapolate these trends over 2030–2060. While prior studies examining the influence of summer temperature increase and boreal fire found an exponential dependence on temperature[25], we utilize a linear increase as a conservative assumption under which boreal emissions remain below observed 2023 annual values until the late 2050s. If the linear extrapolation for a grid cell and month beyond 2023 reaches values below zero, prescribed boreal BBEs in that grid cell and month are set to zero beyond that year – this occurs very seldom and does not impact significantly the overall increase in boreal BBEs in the ramped simulations. Another consequence of the methodology is that future emissions are only prescribed in months and locations with a history of emissions during 1997–2023, which may be a conservative approach (it is possible that future boreal fires may expand, both in seasonality and locations, beyond those observed over 1997–2023). BBEs outside the boreal region are unchanged from CMIP6 forcing and

the model physics are identical to CESM2. We focus our analysis through only 2060, so that even if feedbacks such as the fuel availability negative feedback limit an increase in fire, the prescribed BBEs are precedented. The BBE species that are modified are the same as in past biomass burning senstitivity experiments with CESM2[9,18]. We run an ensemble of 9 members (see Table S1 for details on initial conditions). For comparison to CESM2-LE, we use members 51-100 from the 100-member CESM2-LE, which use a smoothed version of the CMIP6 biomass burning protocol (11-year running means) that is more comparable to the treatment of CMIP6 BMB emissions used before 1997 and after 2014, and thus more directly comparable to the BorealFire ensemble. Conclusions however are unchanged if using CESM2-LE members 1-50 (not shown).

Acknowledgements

EB-W is supported by National Science Foundation OPP ANS grants 2337045 and 2213988. DF is supported by National Science Foundation OPP ANS grant 2337045. PD is funded by the European Union (ERC, ArcticWATCH, 101040858). Views and opinions expressed are however those of PD only and do not necessarily reflect those of the European Union or the European Research Council Executive Agency. Neither the European Union nor the granting authority can be held responsible for them. We thank Steve Warren for insightful comments, analysis, and draft reviews. We would also like to acknowledge high-performance computing support from Cheyenne (doi:10.5065/D6RX99HX) provided by NCAR's Computational and Information Systems Laboratory, sponsored by the National Science Foundation, and CESM2 support from David Bailey.

Author contributions

EB-W analyzed the observed BBEs, designed and produced the model simulations, analyzed the simulation output, and wrote the manuscript. PD helped analyze the observed BBEs, design the model simulations and interpret the output, and edited the manuscript. DF helped interpret the model simulations output, and edited the manuscript.

Competing interests

The authors declare no competing interests.

Materials and correspondence

All correspondence and material requests should be submitted to Edward Blanchard-Wrigglesworth.

Data availability

GFED4s data are available at `https://www.geo.vu.nl/~gwerf/GFED/GFED4/`. NASA MODIS/Aqua aerosol data area available at `https://ladsweb.modaps.eosdis.nasa.gov/missions-and-measurements/products/MYD08_M3`. CESM2-LE data are available via `https://www.cesm.ucar.edu/community-projects/lens2`. Output from the nudged simulations is available at `https://atmos.washington.edu/~ed/data/`.

References

[1] Schmale, J., Zieger, P. & Ekman, A. M. Aerosols in current and future Arctic climate. *Nature Climate Change* **11**, 95–105 (2021).

[2] Haywood, J. & Boucher, O. Estimates of the direct and indirect radiative forcing due to tropospheric aerosols: A review. *Reviews of geophysics* **38**, 513–543 (2000).

[3] McCarty, J. L. *et al.* Reviews and syntheses: Arctic fire regimes and emissions in the 21st century. *Biogeosciences* **18**, 5053–5083 (2021).

[4] Schaepman-Strub, G. & Kim, J.-S. What set siberia ablaze? *Science* **378**, 944–945 (2022).

[5] Li, Y., Janssen, T. A., Chen, R., He, B. & Veraverbeke, S. Trends and drivers of arctic-boreal fire intensity between 2003 and 2022. *Science of the Total Environment* **926**, 172020 (2024).

[6] Huang, X. *et al.* Escalating wildfires in siberia driven by climate feedbacks under a warming arctic in the 21st century. *AGU Advances* **5**, e2023AV001151 (2024).

[7] Chiang, J. C. & Bitz, C. M. Influence of high latitude ice cover on the marine intertropical convergence zone. *Climate Dynamics* **25**, 477–496 (2005).

[8] Jiang, Y. *et al.* Impacts of wildfire aerosols on global energy budget and climate: The role of climate feedbacks. *Journal of Climate* **33**, 3351–3366 (2020).

[9] Fasullo, J. *et al.* Spurious late historical-era warming in CESM2 driven by prescribed biomass burning emissions. *Geophysical Research Letters* **49**, e2021GL097420 (2022).

[10] Clarke, A. D. & Noone, K. J. Soot in the arctic snowpack: A cause for perturbations in radiative transfer. *Atmospheric Environment* **41**, 64–72 (1985).

[11] Fyfe, J. C. *et al.* One hundred years of arctic surface temperature variation due to anthropogenic influence. *Scientific Reports* **3**, 2645 (2013).

[12] Bond, T. C. *et al.* Bounding the role of black carbon in the climate system: A scientific assessment. *Journal of geophysical research: Atmospheres* **118**, 5380–5552 (2013).

[13] Flanner, M. G. Arctic climate sensitivity to local black carbon. *Journal of Geophysical Research: Atmospheres* **118**, 1840–1851 (2013).

[14] Sand, M. *et al.* The arctic response to remote and local forcing of black carbon. *Atmospheric Chemistry and Physics* **13**, 211–224 (2013).

[15] Van Marle, M. J. *et al.* Historic global biomass burning emissions for cmip6 (bb4cmip) based on merging satellite observations with proxies and fire models (1750–2015). *Geoscientific Model Development* **10**, 3329–3357 (2017).

[16] Gidden, M. J. *et al.* Global emissions pathways under different socioeconomic scenarios for use in CMIP6: a dataset of harmonized emissions trajectories through the end of the century. *Geoscientific model development* **12**, 1443–1475 (2019).

[17] Feng, L. *et al.* The generation of gridded emissions data for CMIP6. *Geoscientific Model Development* **13**, 461–482 (2020).

[18] DeRepentigny, P. *et al.* Enhanced simulated early 21st century Arctic sea ice loss due to CMIP6 biomass burning emissions. *Science Advances* **8**, eabo2405 (2022).

[19] Heyblom, K. B., Singh, H. A., Rasch, P. J. & Hirasawa, H. Variability in biomass burning emissions weakens aerosol forcing due to nonlinear aerosol-cloud interactions. *Geophysical Research Letters* **50**, e2022GL102685 (2023).

[20] Garrett, T. J., Brattström, S., Sharma, S., Worthy, D. E. & Novelli, P. The role of scavenging in the seasonal transport of black carbon and sulfate to the Arctic. *Geophysical Research Letters* **38** (2011).

[21] Balcerak, E. Arctic air may become cleaner as temperatures rise. *Eos, Transactions American Geophysical Union* **92**, 360–360 (2011).

[22] Jiao, C. & Flanner, M. G. Changing black carbon transport to the Arctic from present day to the end of 21st century. *Journal of Geophysical Research: Atmospheres* **121**, 4734–4750 (2016).

[23] Jain, P. *et al.* Drivers and impacts of the record-breaking 2023 wildfire season in Canada. *Nature Communications* **15**, 6764 (2024).

[24] Scholten, R. C., Coumou, D., Luo, F. & Veraverbeke, S. Early snowmelt and polar jet dynamics co-influence recent extreme siberian fire seasons. *Science* **378**, 1005–1009 (2022).

[25] Descals, A. *et al.* Unprecedented fire activity above the arctic circle linked to rising temperatures. *Science* **378**, 532–537 (2022).

[26] Luo, B. *et al.* Rapid summer Russian Arctic sea-ice loss enhances the risk of recent Eastern Siberian wildfires. *Nature Communications* **15**, 5399 (2024).

[27] Andela, N. *et al.* A human-driven decline in global burned area. *Science* **356**, 1356–1362 (2017).

[28] Jones, M. W. *et al.* Global and regional trends and drivers of fire under climate change. *Reviews of Geophysics* **60**, e2020RG000726 (2022).

[29] de Groot, W. J., Flannigan, M. D. & Cantin, A. S. Climate change impacts on future boreal fire regimes. *Forest Ecology and Management* **294**, 35–44 (2013).

[30] Sherstyukov, B. & Sherstyukov, A. Assessment of increase in forest fire risk in Russia till the late 21st century based on scenario experiments with fifth-generation climate models. *Russian Meteorology and Hydrology* **39**, 292–301 (2014).

[31] England, M. R., Polvani, L. M., Sun, L. & Deser, C. Tropical climate responses to projected Arctic and Antarctic sea-ice loss. *Nature Geoscience* **13**, 275–281 (2020).

[32] Vavrus, S. J., Holland, M. M., Jahn, A., Bailey, D. A. & Blazey, B. A. Twenty-first-century Arctic climate change in CCSM4. *Journal of Climate* **25**, 2696–2710 (2012).

[33] Boisvert, L. & Stroeve, J. C. The Arctic is becoming warmer and wetter as revealed by the Atmospheric Infrared Sounder. *Geophysical Research Letters* **42**, 4439–4446 (2015).

[34] Kay, J. E. *et al.* Less surface sea ice melt in the CESM2 improves Arctic sea ice simulation with minimal non-polar climate impacts. *Journal of Advances in Modeling Earth Systems* **14**, e2021MS002679 (2022).

[35] Kim, I.-W. *et al.* Abrupt increase in Arctic-Subarctic wildfires caused by future permafrost thaw. *Nature Communications* **15**, 7868 (2024).

[36] Holland, M. M. & Bitz, C. M. Polar amplification of climate change in coupled models. *Climate dynamics* **21**, 221–232 (2003).

[37] Blanchard-Wrigglesworth, E., Armour, K., Bitz, C. M. & deWeaver, E. Persistence and inherent predictability of Arctic sea ice in a GCM ensemble and observations. *Journal of Climate* **24** (2011).

[38] Brown, H. *et al.* Biomass burning aerosols in most climate models are too absorbing. *Nature communications* **12**, 277 (2021).

[39] Helbig, M. *et al.* Boreal forest fire causes daytime surface warming during summer to exceed surface cooling during winter in north america. *AGU Advances* **5**, e2024AV001327 (2024).

[40] Beck, P. S. *et al.* The impacts and implications of an intensifying fire regime on alaskan boreal forest composition and albedo. *Global Change Biology* **17**, 2853–2866 (2011).

[41] Davy, R. & Griewank, P. Arctic amplification has already peaked. *Environmental Research Letters* **18**, 084003 (2023).

[42] Randerson, J., Van Der Werf, G., Giglio, L., Collatz, G. & Kasibhatla, P. Global Fire Emissions Database, Version 4.1 (GFEDv4). ORNL DAAC, Oak Ridge, Tennessee, USA (2018). URL `https://doi.org/10.3334/ORNLDAAC/1293`. Updated 2023.

[43] Van Der Werf, G. R. *et al.* Global fire emissions estimates during 1997–2016. *Earth System Science Data* **9**, 697–720 (2017).

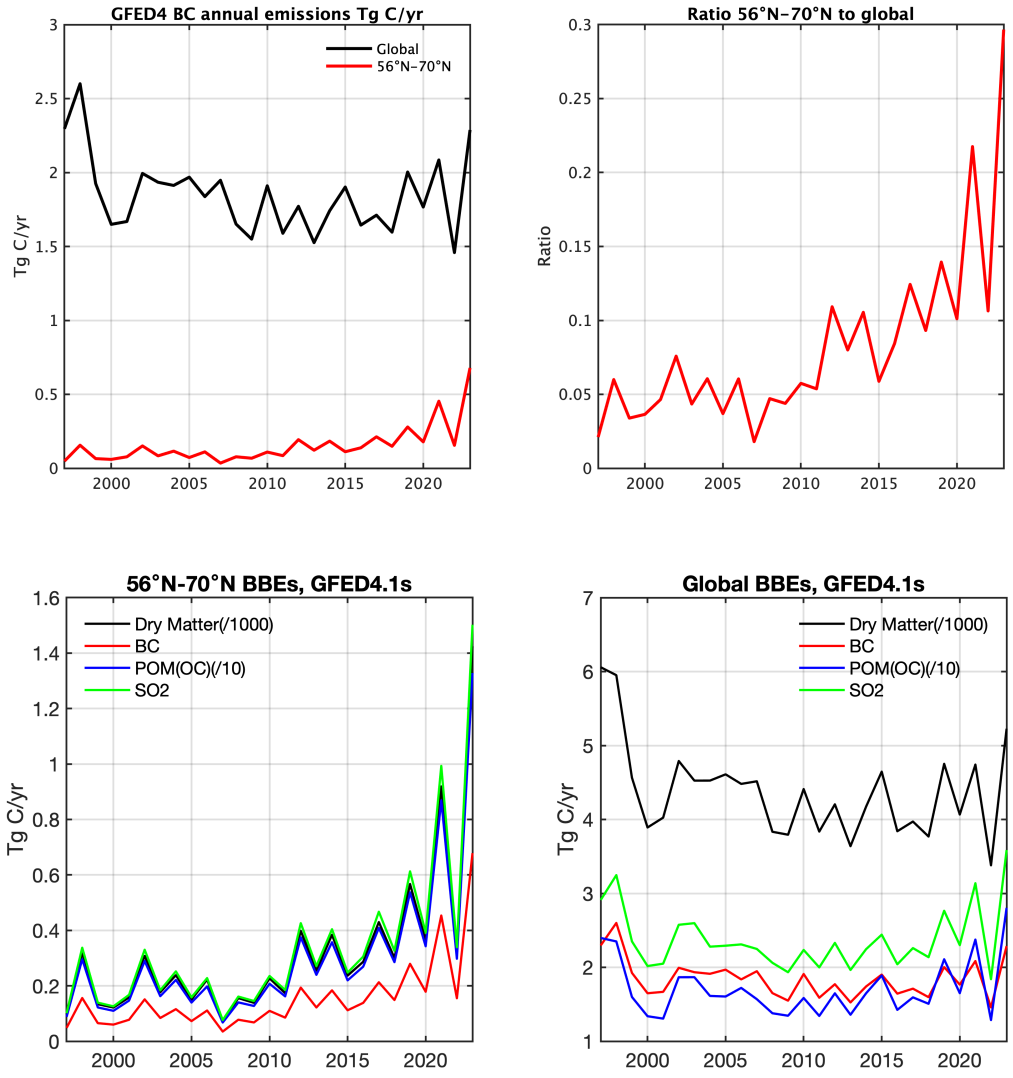
[44] Danabasoglu, G. *et al.* The community earth system model version 2 (cesm2). *Journal of Advances in Modeling Earth Systems* **12**, e2019MS001916 (2020).

[45] Rodgers, K. B. *et al.* Ubiquity of human-induced changes in climate variability. *Earth System Dynamics* **12**, 1393–1411 (2021).

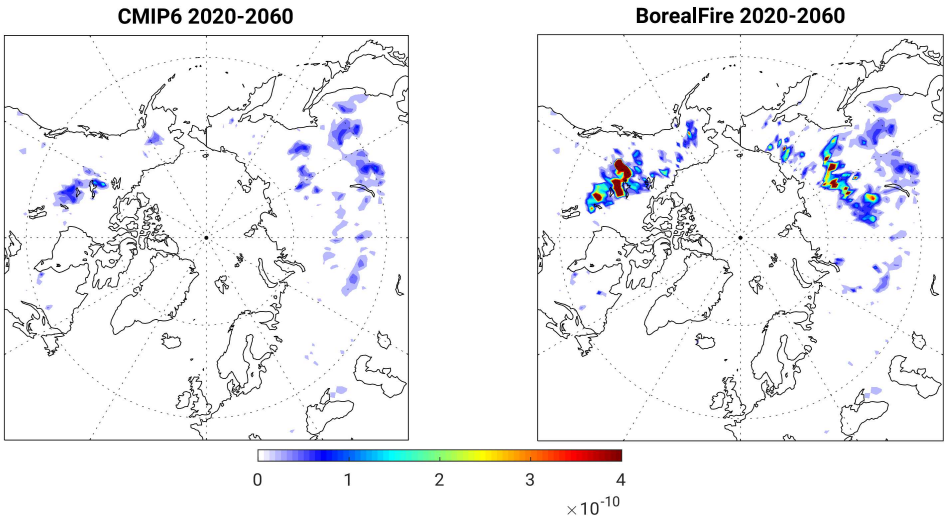
Table 1: Summary of BorealFire model simulations.

Run ID	Initial conditions	IC experiment	forcing, years
BorealFire01	b.e21.BHIST.f09_g17.CMIP6-historical.001	CMIP6	CMIP6, 2015-2060
BorealFire02	b.e21.BHIST.f09_g17.CMIP6-historical.002	CMIP6	CMIP6, 2015-2060
BorealFire03	b.e21.BHISTcmip6.f09_g17.LE2-1001.001	CESM2-LE	CMIP6, 2015-2060
BorealFire04	b.e21.BHISTcmip6.f09_g17.LE2-1231.001	CESM2-LE	CMIP6, 2015-2060
BorealFire05	b.e21.BHISTcmip6.f09_g17.LE2-1251.001	CESM2-LE	CMIP6, 2015-2060
BorealFire06	b.e21.BHISTcmip6.f09_g17.LE2-1281.001	CESM2-LE	CMIP6, 2015-2060
BorealFire07	b.e21.BHISTsmbb.f09_g17.LE2-1011.001	CESM2-LE	CMIP6, 2015-2060
BorealFire08	b.e21.BHISTsmbb.f09_g17.LE2-1231.011	CESM2-LE	CMIP6, 2015-2060
BorealFire09	b.e21.BHISTsmbb.f09_g17.LE2-1251.011	CESM2-LE	CMIP6, 2015-2060

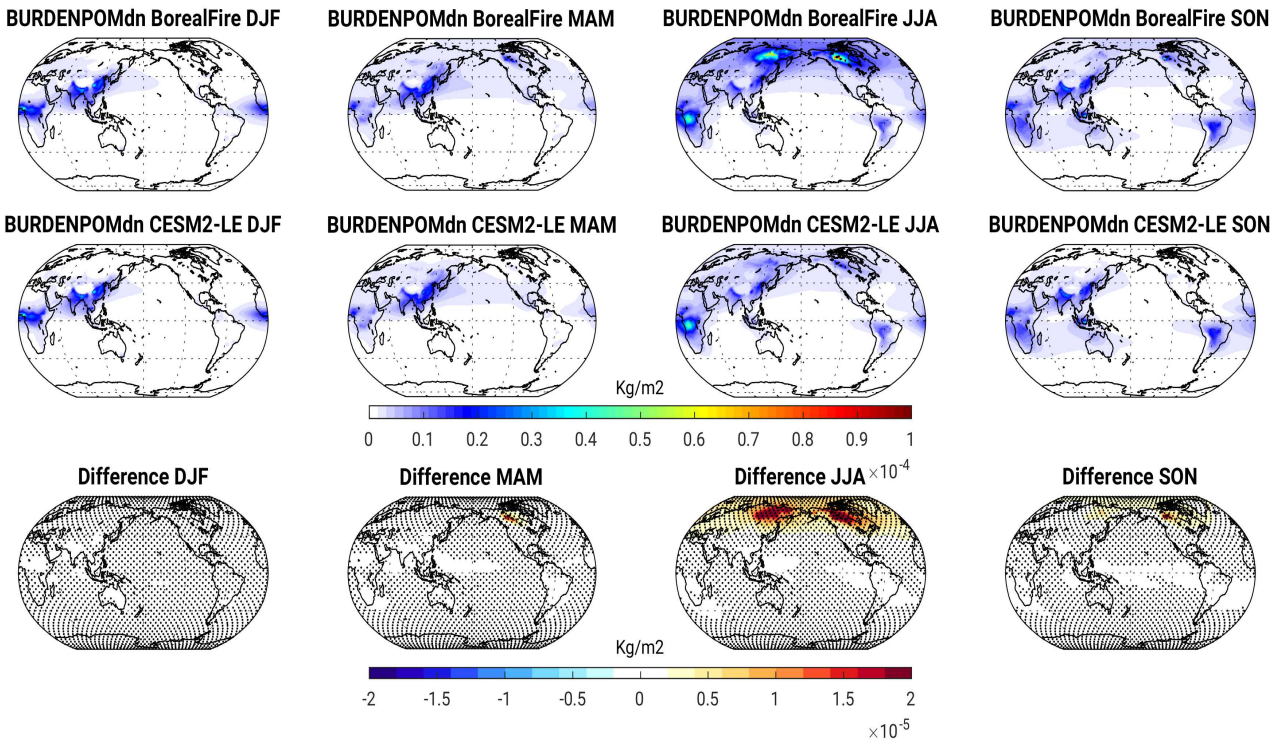
Supplementary Information



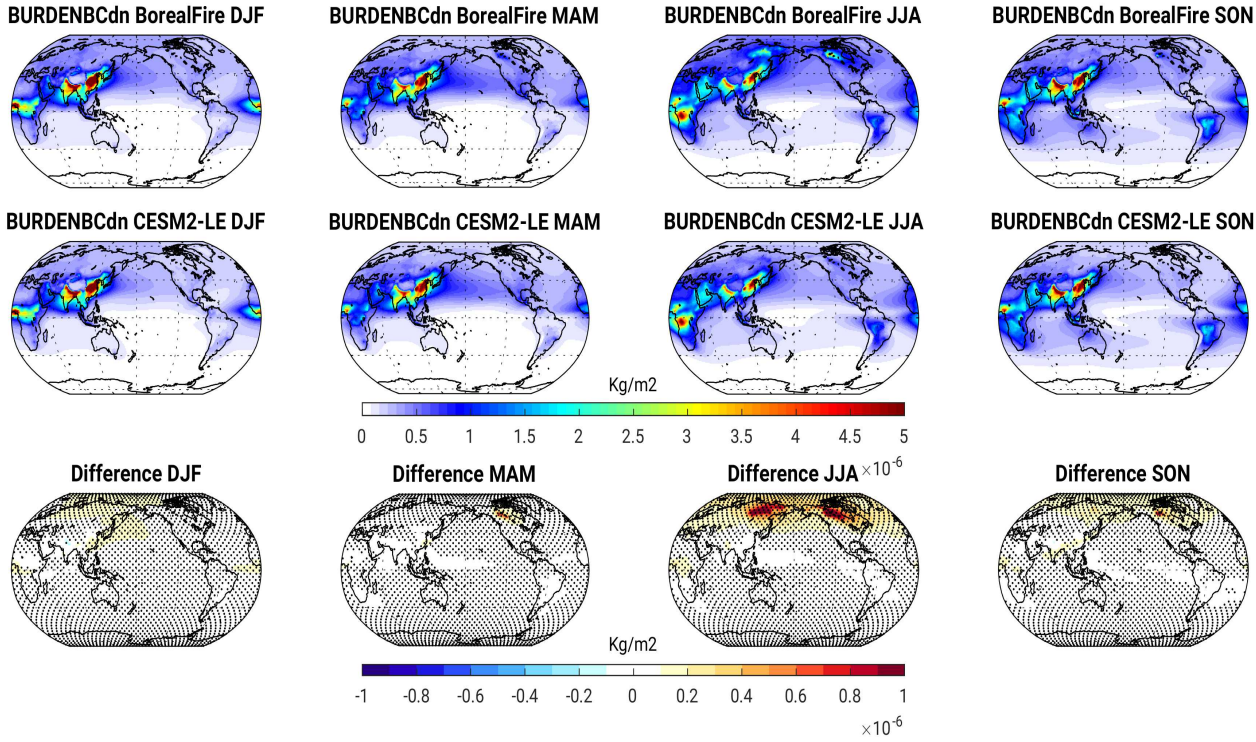
Supplementary Fig. 1 | (A) Global (black) and boreal (red) (56°N–70°N) BC from BBEs in GFED4s and (B) their ratio. (C) Boreal BBEs of total dry matter (/1000, black), BC (red), SO2 (green), POM (/10, blue), and (D) as in (C), for global BBEs.



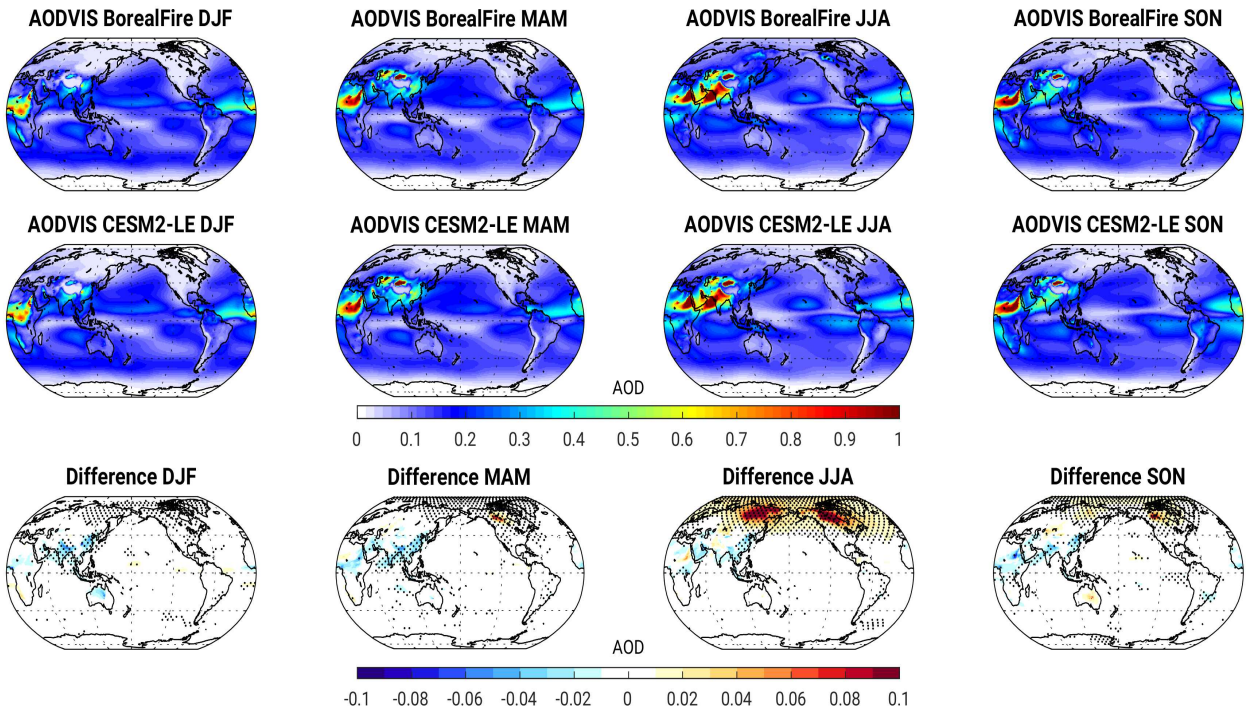
Supplementary Fig. 2 | Mean spatial boreal BC from BBEs in kg/m^2 over 2020–2060 in (A) CMIP6 forcing and (B) BorealFire.



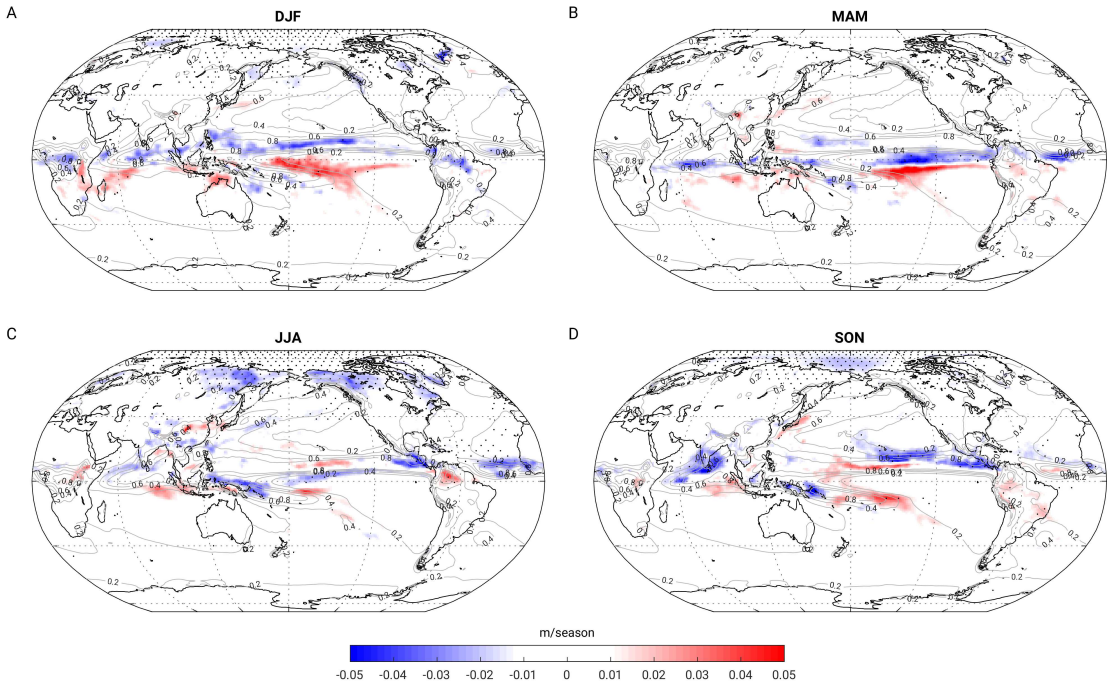
Supplementary Fig. 3 | Mean seasonal primary organic matter (POM) burden in BorealFire (top row), CESM2-LE (middle row), and the difference between the two (bottom row).



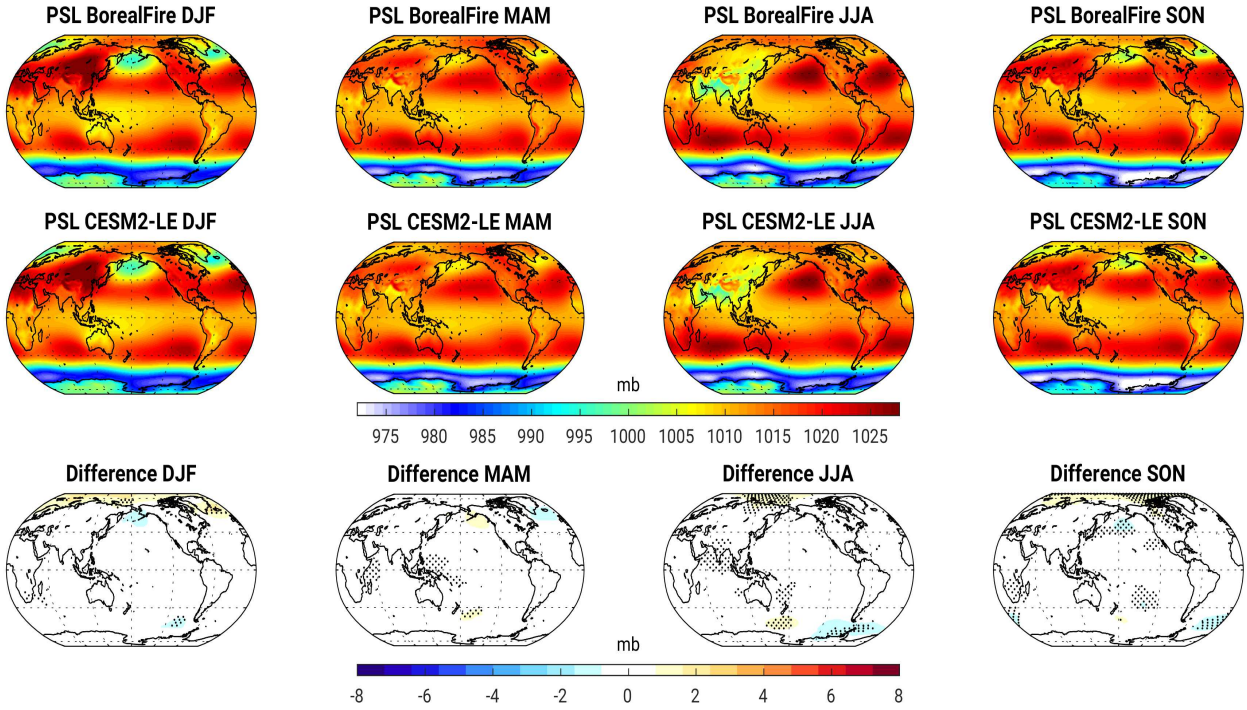
Supplementary Fig. 4 | As for Supplementary Fig. 3, but for BC burden.



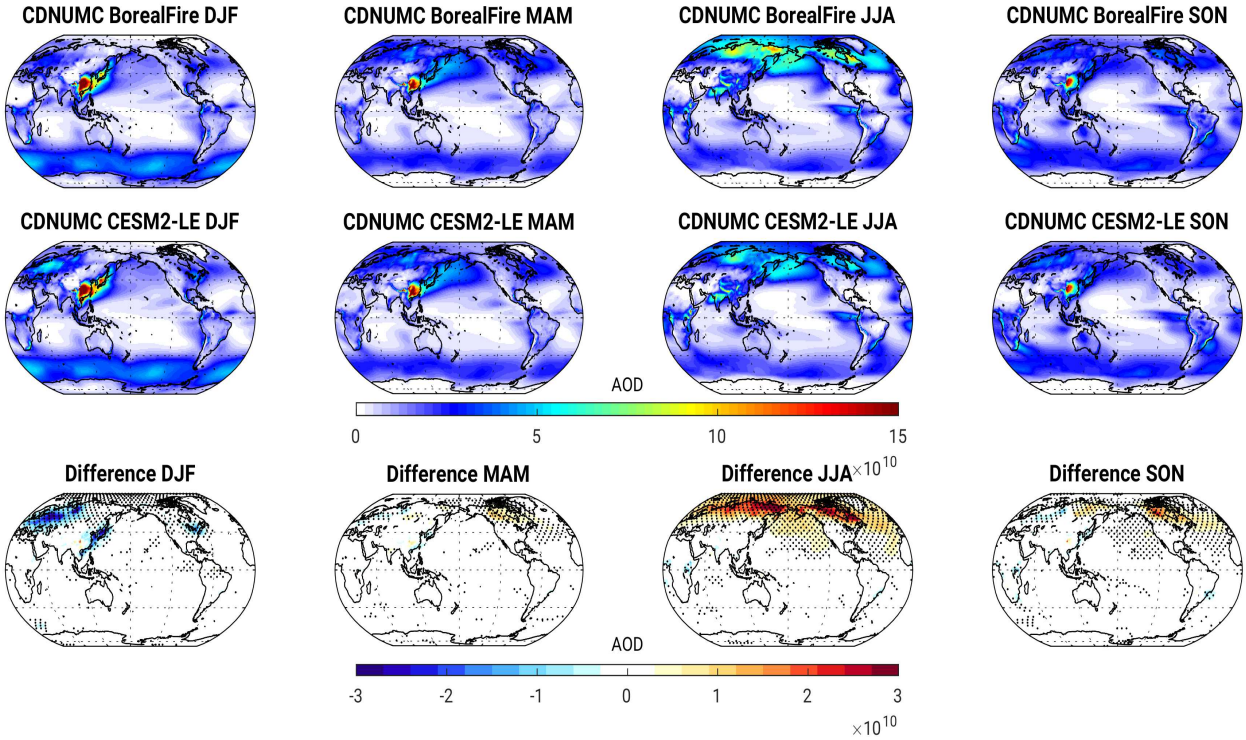
Supplementary Fig. 5 | As for Supplementary Fig. 3, but for aerosol optical depth (AOD).



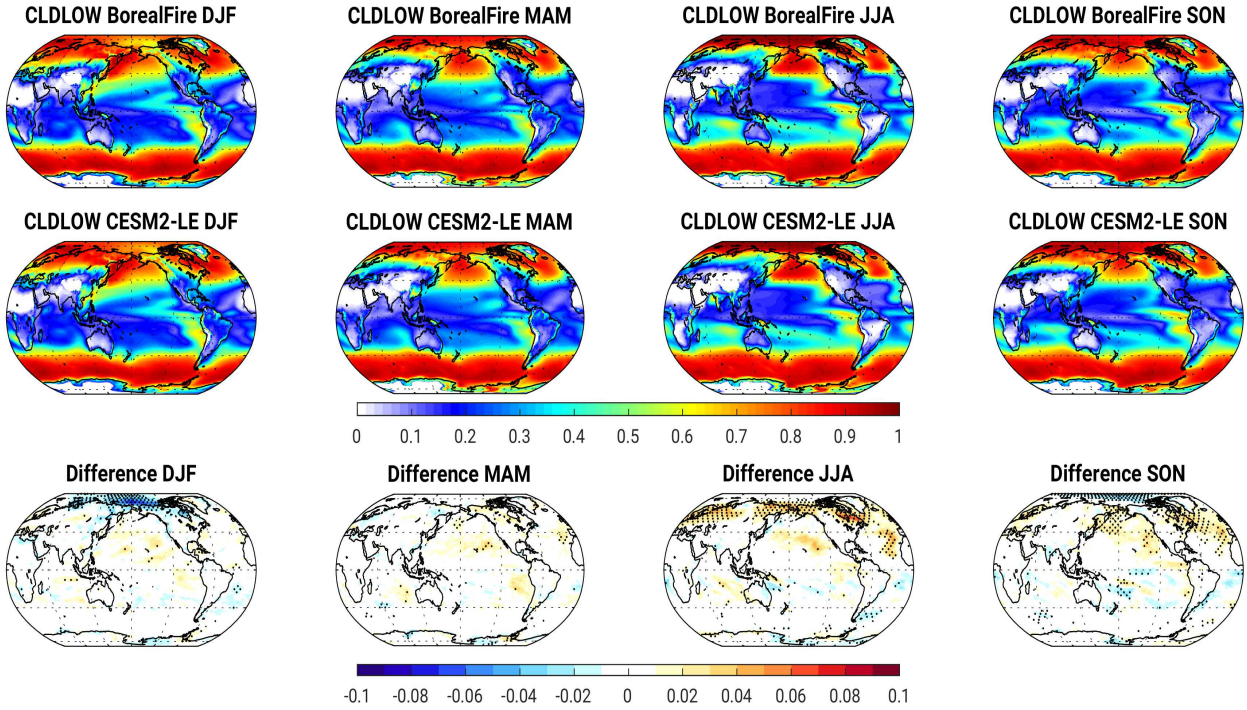
Supplementary Fig. 6 | Seasonal changes in precipitation between BorealFire and CESM2-LE.



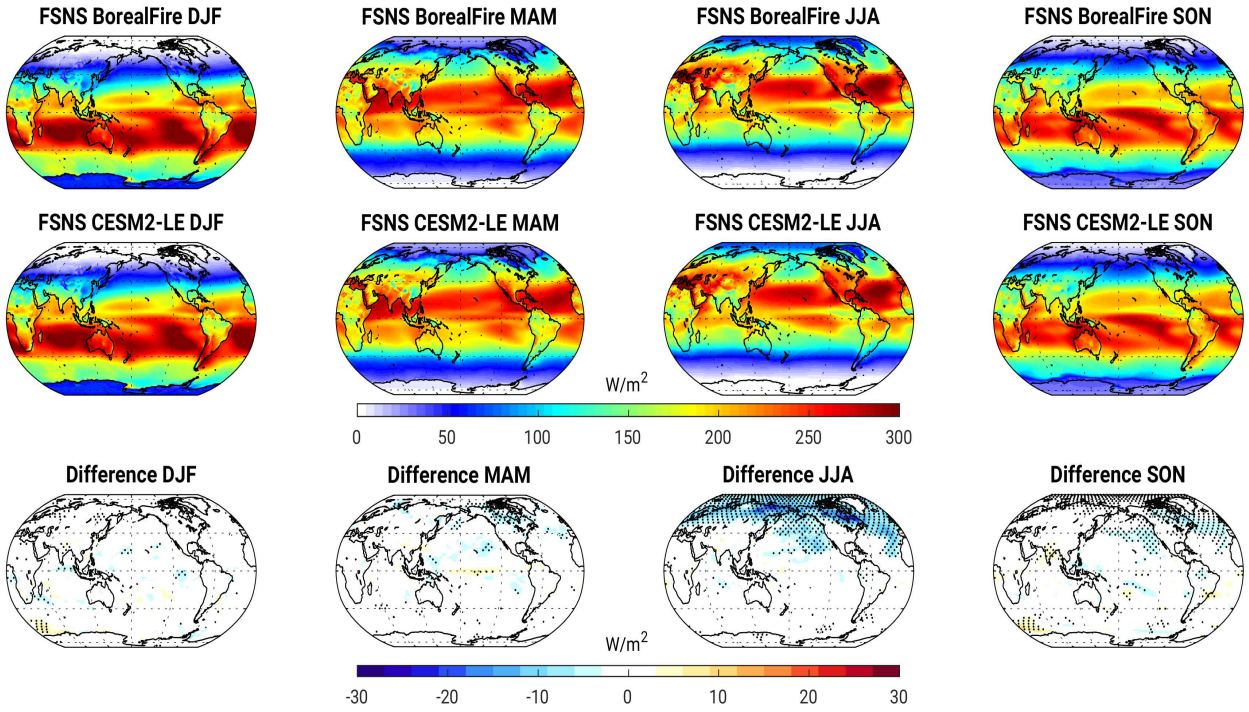
Supplementary Fig. 7 | As for Supplementary Fig. 5, but for sea-level pressure.



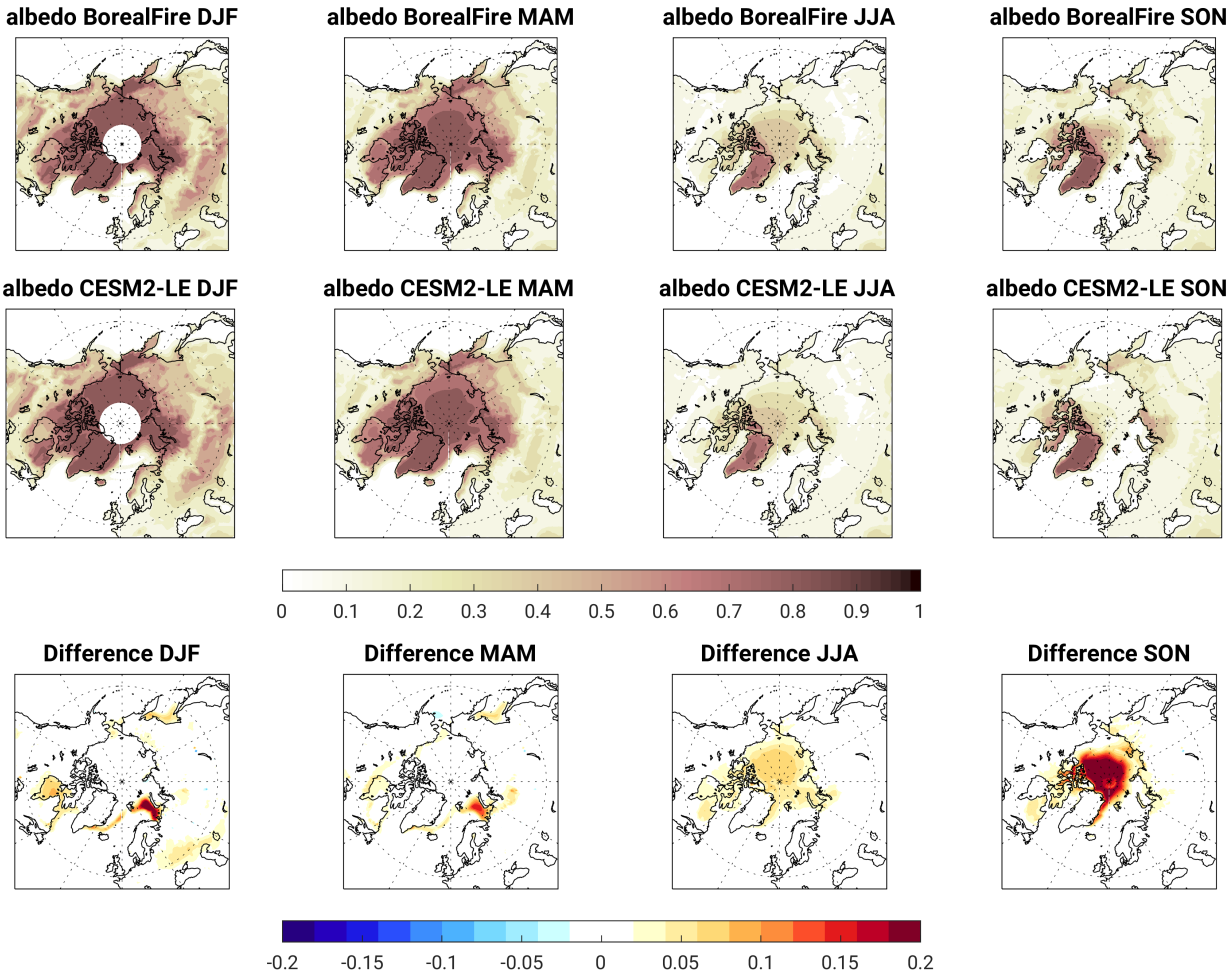
Supplementary Fig. 8 | As for Supplementary Fig. 5, but for cloud droplet number.



Supplementary Fig. 9 | As for Supplementary Fig. 5, but for low cloud cover.



Supplementary Fig. 10 | As for Supplementary Fig. 5, but for net surface shortwave flux (FSNS).



Supplementary Fig. 11 | As for Supplementary Fig. 5, but for surface albedo.